# Investigation of Endmilled Accuracy under a Constant Cutting Speed Vector Considering Approach Path with a Five Axis Controlled Machine Tool

Honoka Tabata*, Toshiki Hirogaki, and Eiichi Aoyama

Manufacturing System and Design Laboratory, Doshisha University, 1-3 Tatara Miyakodani, Kyotanabe-shi, Kyoto-fu, Japan
Email: synniht14s@gmail.com (H.T.); thirogak@mail.doshisha.ac.jp (T.H.); eaoyama@mail.doshisha.ac.jp (E.A.)
*Corresponding author

Manuscript received April 4, 2023; revised June 6, 2023; accepted August 3, 2023; published January 2, 2024

***Abstract*—In simultaneous 5-axis end milling, when creating a curved surface, it is difficult to achieve consistent quality of the machined surface. However, it is known that the machine behavior changes when the approach is changed. Hence, this study aims to demonstrate the usefulness of the constant cutting point feed rate vector condition by conducting cutting experiments considering the approach. In addition, we devise a machining path to create a circle and propose an optimization method for corner tolerance speed difference. With this technique, the roundness value can be reduced by 37.2%, and a circle with a cleaner shape than the original can be machined.**

***Keywords*—five-axis machining center, synchronous motion, shape error, higher-precision**

## I. Introduction

In recent years, 5-axis control machining centers equipped with linear and swivel axes have become remarkably popular. This is not only because of jigless machining, which uses the motion of the swivel axis for indexing, but also because simultaneous control using the linear and swivel axes enables the machining of complex shapes where the tool and workpiece interfere with each other using a 3-axis MC [1–3]. However, in machining technology, shape accuracy, such as free-form surfaces, and surface quality, such as uniformity of roughness across the entire created surface, may be particularly important. To achieve this, it is necessary to maintain a constant relative feed rate between the end mill and the workpiece at the cutting point (hereinafter referred to as the cutting point feed rate). However, in conventional machining using circular interpolation motion with simultaneous control of two linear axes using an endmill on a 3-axis machine tool, the tool center feed rate (feed command value in the NC program) and cutting point feed rate are different. Therefore, in the previous report [3], we proposed a method for a constant feed rate vector at the cutting point in the end milling of a 2-dimensional circular arc shape by simultaneous 3-axis control with two straight axes and one swivel axis using a 5-axis MC. The results showed that the direction parallel to the vector direction of the cutting point feed rate has the advantage that errors due to machine tool motion accuracy and thermal deformation are not transferred to the machined shape, and the orthogonal direction has the feature that the positive and negative directions of error transfer are reversed [4]. Moreover, we discussed the influence of motion performance in a rotary axis on motion accuracy under a constant feed rate vector condition [5]. However, the factors of machining errors caused by the differences in the characteristics of the servo system resulting from the synthesis of rotary axis motion with linear axis motion have not yet been clarified, and improvement methods have not yet been investigated. In a previous study, we focused on the motion of cutting a circular shape using a constant cutting point feed rate method with two linear axes and one rotary axis of a 5-axis MC, and investigated the error factors affecting the machined shape. It was found that the shape error is caused by the relative angle difference, which is the difference between the radius reduction of the straight axis and the phase delay from the command value of the swivel and straight axes. Therefore, we considered reducing the relative angle difference to zero to decrease the shape error. It is known that changing the approach changes the behavior of the machine [6]. The purpose of this study was to demonstrate the usefulness of the constant cutting point feed rate vector condition by conducting cutting experiments that consider this approach. This study focuses on the corner allowable speed difference in the linear approach motion when cutting a circular shape to reduce the shape error.

## II. Basic Theory

The constant cutting point feed rate method is illustrated in Fig. 1. It represents a state in which the magnitude and direction of the cutting point feed rate at cross-section P - P' are always constant during one scan of the tool around the workpiece in contour machining. To realize this, the rotation of the workpiece fixed on the swivel table is required. If $\omega_R$ rad/s is the C-axis rotation angular velocity, $R_W$ mm is the offset between the C-axis rotation center and the center of curvature axis $O_W$, and $F_C$ mm/min is the cutting-point feed rate. The C-axis rotation angular velocity $\omega_R$ rad/s is given by Eq. (1).

$$\omega_R = F_C / (60 R_C) \tag{1}$$

where $R_C$ mm is the radius of curvature of the cross-section perpendicular to the center axis of curvature $O_W$. The command feed rate $F$ mm/min of the tool center axis in the

DOI: 10.7763/IJMO.2024.V14.842

machine coordinate system when the worktable is horizontal (B axis= 90[°]) can be expressed using (2).

$$F = 60 R_W \omega_R \tag{2}$$

By substituting Eq. (1) into Eq. (2), the relationship in equation (3) can be established.

$$F : F_C = R_W : R_C \tag{3}$$

From Eq. (3), the angular velocity $\omega_L$[rad/s] of the straight axis is always $\omega_L = \omega_R$ (hereafter, $\omega_L = \omega_R = \omega$) [4].

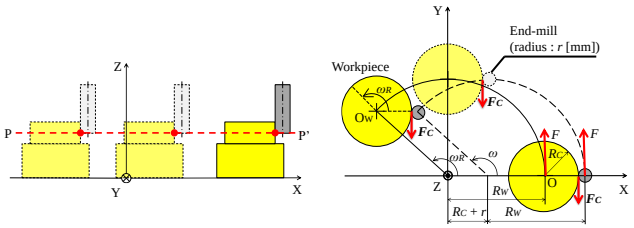


(a) (b)

Fig. 1. Constant feed speed vector of milling point. (a) X-Z plane. (b) X-Y plane (P-P' section).

## III. Experimental Device

A trunnion-type 5-axis vertical multitasking machine (Super MILLER 400, DMG Mori Seiki) shown in Fig. 2, was used as the experimental setup. A two-flute square end mill (Mitsubishi Materials C2MAD0600) with a tool radius of $r$ = 3 [mm] and torsional angle of 37.5° was used. Before the cutting experiment, the center of the swivel C-axis and origin of the X-Y-axis were aligned using a lever-type differential transformer-type electric micrometer E-DT-LM-S30 (manufactured by Tokyo Seimitsu). As shown in Fig. 3, the micrometer fixed to the work table was applied to the end mill and the axes were adjusted until the micrometer gauge no longer exceeded ±1μm when one revolution was made along the table.

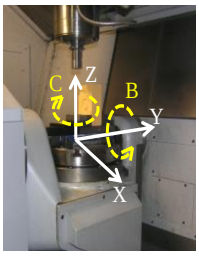


Fig. 2. Five-axis machine tool.

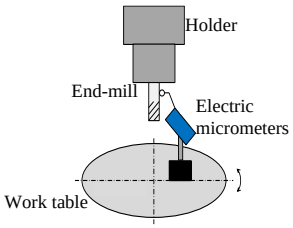


Fig. 3. Axis adjustment.

A servo adjustment tool (SERVO GUIDE, FANUC) was used to obtain scale values inside the machine. From the starting position, the displacement was measured in millimeters for the straight axis and the rotation was measured in degrees for the swivel axis with the a positive CCW direction. A wireless holder (4K-WISY, ARTIS, sampling period 2kHz) was used to measure the cutting force during the experiments, as shown in Fig. 4. The directional relationship between the holder and measurement results is shown in Fig. 5. To measure the roundness of the workpiece, a roundness measuring instrument, RONCORDER EC600 (Kosaka Laboratory) was used.

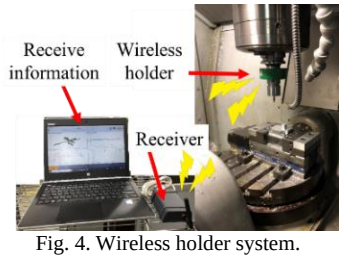


Fig. 4. Wireless holder system.

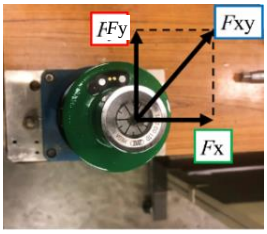


Fig. 5. Direction of each force.

## IV. Experimental Method

The cylindrical workpiece shown in Fig. 6 was cut under a constant cutting-point feed rate vector condition. The command radius under the constant cutting-point feed rate condition was set to 60 mm, and the vector direction was parallel to the Y-axis in the negative direction and downcut. The position loop gains $K_{pp}$ for the straight and swivel axes were set to $K_{pp}$ = 60 [1/s] (default setting).

The machining approach paths used are illustrated in Fig. 7. The processing conditions are presented in Table 1. To set the cutting-point feed rate $F_C$ mm/min to 1131, the commanded feed rate $F$ mm/min was set according to the size of the curvature radius $R_C$ using (1).

(a) Although the swivel axis was 90° aided, the tool was intruded 94.2 mm from the negative Y-axis direction in a linear motion to make one rotation of the swivel axis and tool simultaneously. Then, when the swivel axis was moved at 90° again, the tool was withdrawn in a 94.2 mm straight-line motion in the positive direction of the Y-axis. This is known as straight-line path with a running start.

(b) The straight-line motion of the tool in (a) was changed to a pseudo-linear motion with an arc motion and a very large radius of curvature. The length of the approach path of the straight axis was adjusted to 30π mm. The starting point of the cutting was set to ($X_X$, $Y_X$), and the X coordinate of the starting point of the tool was set to $X_X$-1. Therefore, the Y coordinate was $Y_X$-94, and the approach radius $R_f$ = 4172.5[mm] was set for cutting. This is referred as a pseudo-straight- line path with a running start.

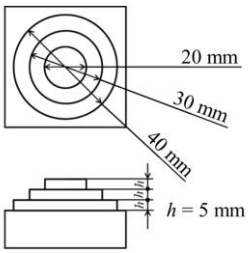


Fig. 6. Workpiece.

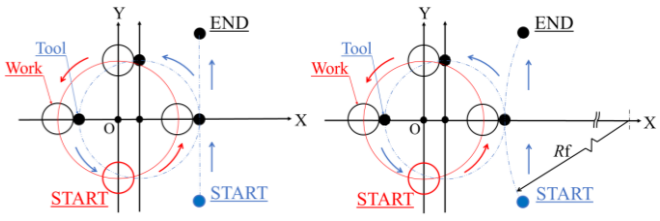


(a) (b)

Fig. 7. Model of machining path. (a) Straight-line path with a running start. (b) Pseudo-straight-line path with a running start.

Table 1. Cutting conditions

| Curvature radius $R_c$ [mm] | 10 | 15 | 20 | Straight |
|---|---|---|---|---|
| Tool radius $r$ [mm] | 3 | | | |
| Helix angle of tool [deg.] | 37.5 | | | |
| Number of cutting edge | 2 | | | |
| Workpiece | Aluminum | | | |
| Command radius $R_w$ [mm] | 60 | | | |
| Spindle speed $S$ [min$^{-1}$] | 9000 | | | |
| Cutting-point feed rate $F_c$ [mm/min] | 1131 | | | |
| Commanded feed rate $F$ [mm/min] | 6786 | 4524 | 3393 | 1131 |
| Radius depth of cut [mm] | 0.5 | | | |
| Coolant | Dry air | | | |

## V. Experimental Results and Discussion

### A. Relationship between Time and Velocity of Each Axis

Fig. 8 shows the relationship between time and cutting resistance $F_{xy}$, where the cylindrical shape shown in Fig. 6 was cut using the machining path shown in Fig. 7. All the data used were for a radius of curvature $R_C$ = 20 [mm]. First, we consider the path in (a). The command feed rate was set at 1131 mm/min =18.8 min/s for assisting and 3393 mm/min =56.6 mm/s for cutting. However, based on the data obtained from the actual servo, the speeds were 12.5 to 13.5 mm/s during the assisting phase and 55.3 to 56.9 mm/s during the cutting phase. The command feed rate during the auxiliary run did not reach the set value. By constant, we consider the path in (b). As in (a), the command feed rate was set to 18.8 min/s during the assisting phase and 56.6 mm/s during the cutting phase. The data obtained from the actual servo showed that the speeds were 18.6 to 19.2 mm/s during the auxiliary run and 56.2 to 56.8 mm/s during the cutting run. The command feed rate was at the set value during both the assisting run and cutting.

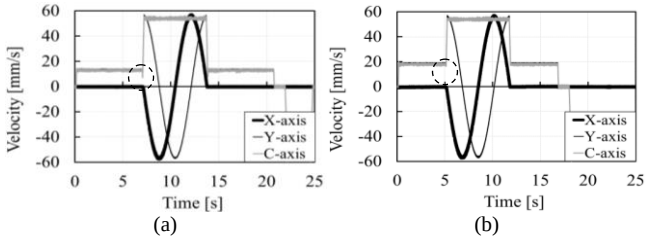


Fig. 8. Relationship between Time and Velocity by machining path. (a) Straight-line path with a running start. (b) Pseudo-straight-line path with a running start.

An enlarged view of the graph in Fig. 8 is shown in Fig. 9. As can be observed, (a) decelerates from approximately 13.5 mm/s to 7.1 mm/s (approximately 47%). In contrast, (b) shows acceleration without deceleration.

### B. Feed Rate when Using Linear Interpolation and Swivel A-axis Simultaneously

In section A, the commanded feed rate at the start and end of cutting did not reach the set value in (a); however, it reached the set value in (b). This indicates that the feed rate changes depending on whether the swivel A-axis is used during the auxiliary run and at the end of cutting. Therefore, if the swivel A-axis is used in linear interpolation, the following formula is calculated if the command feed rate in NC is $F_{real}$. By assuming that the travel distance to the Y-axis = $Y$ [mm] and the swivel angle of the A-axis A [°] = A [mm], we obtain the following equations.

$$L = \sqrt{Y^2 + A^2} \tag{4}$$

$$F_{real} = F \times Y / L \tag{5}$$

In this case, $Y$ = 94.2 [mm] and $A$ = 90 [mm]; thus $F_{real}$ = 818 [mm/min] = 13.6 [mm/s]. Comparing this with the feed rate $V$ = 12.5 to 13.5 [mm/s] obtained from the servo, we see that it is almost the same. Therefore, it is conceivable that this calculation method was used for the actual command feed rate. The machining conditions are shown in Table 2. Cutting is performed with the set value $F$ = 1564 [mm/min] so that the NC command feed rate $F_{real}$ = 1131 [mm/min].

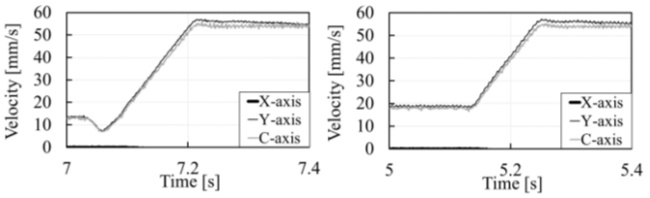


Fig. 9. Relationship between Time and Velocity by machining path (enlarged version). (a) Straight-line path with a running start. (b) Pseudo-straight-line path with a running start.

Table 2. Cutting Conditions

| Curvature radius $R_c$ [mm] | 10 | 15 | 20 | Straight |
|---|---|---|---|---|
| Tool radius $r$ [mm] | 3 | | | |
| Helix angle of tool [deg.] | 37.5 | | | |
| Number of cutting edge | 2 | | | |
| Workpiece | Aluminum | | | |
| Command radius $R_w$ [mm] | 60 | | | |
| Spindle speed $S$ [min$^{-1}$] | 9000 | | | |
| Cutting-point feed rate $F_c$ [mm/min] | 1131 | | | |
| Commanded feed rate $F$ [mm/min] | 6786 | 4524 | 3393 | 1564 |
| Radius depth of cut [mm] | 0.5 | | | |
| Coolant | Dry air | | | |

### C. Prevention of Deceleration During Circular Cutting when Cutting in Straight-line Path with a Running Start

In section A, when cutting in (a), there was a significant deceleration during the circular cutting. To prevent this, the leading control G08P1Q4 (SHG adjustment parameter), as shown in Table 3, was used. Previously, the parameter value of Q3 was used; however, this time Q4 was used and only the values of the corner allowable speed difference $\Delta V$ were changed to 200 (initial value), 416, and 600 for cutting.

Table 3. Shg adjustment parameter

| | Q1 | Q2 | Q3 | Q4 | Q5 |
|---|---|---|---|---|---|
| Acceleration/deceleration time constant after interpolation [ms] | 32 | 32 | 32 | 32 | 32 |
| Upper limit of feed rate at arc radius $R$ [mm/min] Reference radius $R$= 5.000 | 3500 | 5000 | 2000 | 2000 | 2000 |
| Lower limit of arc feedrate | 2000 | 2000 | 2000 | 2000 | 2000 |

| clamp[mm/min] | | | | | |
|---|---|---|---|---|---|
| SHG1:Acceleration/deceleration time constant before interpolation [ms] Standard cutting feed rate *F* 10000 | 320 | 160 | 400 | 400 | 400 |
| SHG1: Corner allowable speed difference [mm/min] | 200 | 48 | 200 | 200 | 200 |

Fig. 10 shows a magnified version of the relationship between time and velocity near the start of cutting. From this, the larger the value of the corner allowable speed difference $\Delta V$, the more deceleration is suppressed. When the speed exceeded 416 mm/min, the acceleration decreased during the middle of the process. Therefore, 416 mm/min was selected as the optimum speed because it allowed for reduced deceleration and constant acceleration.

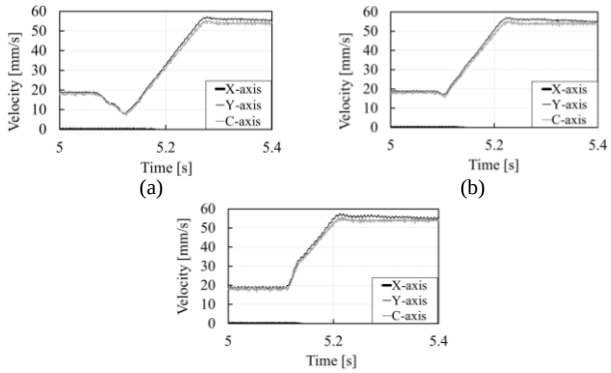


Fig. 10. Relationship between time and velocity for each value of the corner allowable speed difference $\Delta V$ (Enlarged version). (a) 200 mm/min; (b) 416 mm/min; (c) 600 mm/min.

Fig. 11 shows the trajectories of the X and Y-axis near the start and end of cutting. It can be observed that the curves are cleaner at 416 mm/min (optimum value) and 600 mm/min (beyond the optimum value) than at 200 mm/min (initial value). Therefore, it is considered that the actual cut shape is better when the deceleration of the Y and C-axis is suppressed near the start and end of cutting.

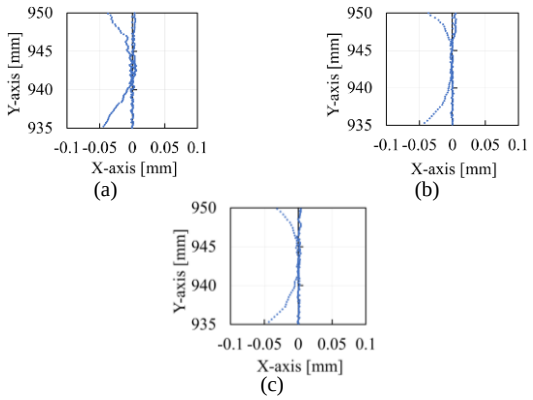


Fig. 11. X and Y axis trajectories for each value of the corner allowable speed difference $\Delta V$. (a) 200 mm/min; (b) 416 mm/min; (c) 600 mm/min.

Furthermore, Fig. 12 shows the relationship between time and cutting force norm $F_{xy}$. At 200 mm/min, the cutting resistance was low after the start of cutting. However, it was slightly suppressed at 416 mm/min and 600 mm/min. Low frequencies were observed during the circular cutting at 200 mm/min and 600 mm/min, but were constant at 416 mm/min compared to the others.

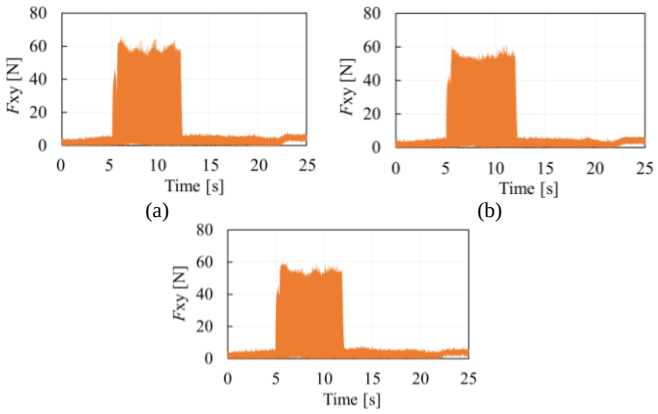


Fig. 12. Relationship between time and $F_{xy}$ for each value of the corner allowable speed difference $\Delta V$. (a) 200 mm/min; (b) 416 mm/min; (c) 600 mm/min.

Finally, Fig. 13 presents a graph of the roundness of the cut workpiece. The roundness values at 200 mm/min, 416 mm/min, and 600 mm/min were 8.6, 5.4, and 9.3 μm, respectively, indicating that the roundness was smallest at 416 mm/min (when the optimum value was used), 37.8% smaller than at 200 mm/min (initial value). The shape of the graph shows depressions near the start and end of the cutting at 200 and 600 mm/min. Furthermore, at 600 mm/min, an overall runout occurred. It is assumed that the tool vibrates during the cutting. Therefore, the corner allowable speed difference of 416 mm/min (optimum value) is considered to be the most advantageous.

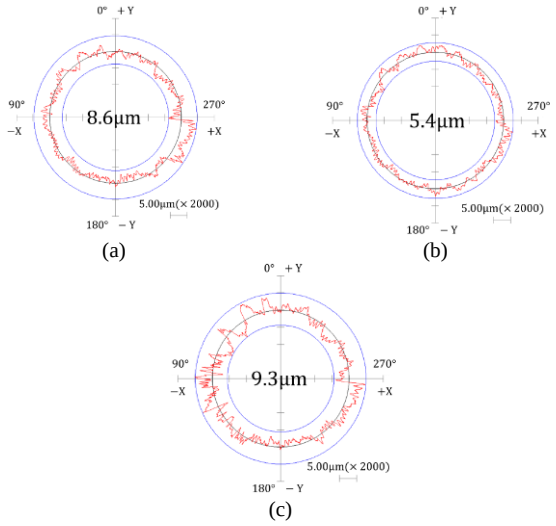


Fig. 13. Roundness for each value of the corner allowable speed difference $\Delta V$. (a) 200 mm/min; (b) 416 mm/min; (c) 600 mm/min.

## VI. Conclusion

This study focused on the motion of circular shape cutting under the "constant cutting point feed rate condition" using two linear axes and one swivel axis of a 5-axis control machine tool. Two machining approach paths were proposed. One was a straight-line path with a running start and the other was a pseudo-straight-line path with a running start. Both paths ran along a straight line. However, there were differences between the two paths, one using linear interpolation and the other using circular interpolation. Cutting experiments were conducted using these paths and

the cutting resistance and roundness of the workpiece were measured. Consequently, we determined the following.

1. The actual feed rate of the pseudo-linear path with a running start was almost the same as the set command feed rate; however, the actual feed rate of the straight path with a running start did not reach the set command feed rate. This is because NC recalculated the feed rate using a certain calculation method. Determining the command value by considering the calculation method in advance is sufficient.
2. The straight-line path with the aid decelerates at the start of the cutting. This deceleration can be prevented by changing the value of the "corner allowable speed difference" to an optimal value. Subsequently, by cutting at the optimum value, the cutting resistance is kept constant and the roundness of the workpiece can be reduced. This time we were able to reduce the size by 37.8%.

## Conflict of Interest

The authors declare no conflict of interest.

## Author Contributions

H. Tabata conducted the research; Toshiki Hirogaki analyzed the data; Eiichi Aoyama wrote the paper; all authors had approved the final version.

## Acknowledgment

I would like to thank T. Hirogaki and E. Aoyama for useful discussions. I wish to thank Manufacturing System and Design Laboratory for advice on experimental design.

## References

[1] S. Natsume, K. Nakamoto, T. Ishida, and Y. Takeuchi, "Highly efficient semi-finishing machining by simultaneous 5-Axis controlled machining using square end mills," *Transactions of the Japan Society of Mechanical Engineers*, Part C, vol. 78, no. 793, pp. 3305–3316, 2012 (in Japanese).

[2] I. Tsuji, K. Kawasaki, Y. Abe, and H. Korihara, "Study on machining method of large spiral bevel gears by general purpose multi-axis control machine tools," *Transactions of the Japan Society of Mechanical Engineers*, Part C, vol. 77, no. 775, pp. 728–736, 2011(in Japanese).

[3] T. Hirogaki, E. Aoyama, K. Ogawa, F. Kawaguchi, and T. Horiuchi, "A study on endmill tool path under constant cutting point feed rate vector condition by 5-Axis control machining center," *Journal of Japan Society for Precision Engineering*, vol. 76, no. 8, pp. 912–917, 2010(in Japanese).

[4] T. Suzuki, I. Takakazu, A. Takayuki, H. Toshiki, A. Eiichi, and O. Keiji, "Motion tuning method of linear axes and rotary axis under a constant cutting speed vector at end-milling point with a five-axis controlled machining center," *ASME*, V02BT02A048, 2015.

[5] T. Suzuki, K. Yoshikawa, T. Hirogaki, E. Aoyama, and T. Ikegami, "Improved method for synchronizing motion accuracy of linear and rotary axes under a constant feed speed vector at the endmilling point," *Journal of Automation Technology*, vol. 13, no. 5, pp. 679–690, 2019.

[6] L. Tapic, K. B. Mawussi, B. Anselmetti, "Circular tests for HSM machine tools: Bore machining application," *International Journal of Machine Tools & Manufacture*, vol. 47, pp. 805–819, 2007.